asteroids is 43, 120, and 194, respectively (Fig. 1); it is clear that the higher the ejection velocity, the greater the number of asteroids that can supply meteoroids to the escape channel. Because there are no known processes that would lead to extensive intermixing of diverse asteroids near the center of the Asteroid Belt, it seems likely that there are relatively few classes of iron meteorites near the 1:3 resonance. In addition, most asteroids may have silicates on their surfaces; thus, this comparison of the number of asteroids that can be sampled probably overestimates the diversity of iron meteorites that this mechanism could yield.

The second escape channel involves perturbations of meteoroids into Earth-crossing orbits resulting from close encounters with Mars (*17, 19*). Williams and Hierath (*20*) noted that 3% of the small PLS (Palomar-Leiden Survey) asteroids have perihelia that during some epochs are inside the aphelion of Mars; a much larger fraction have perihelia within a few tenths of an astronomical unit of the martian orbit. There are two reasons why a greater diversity of iron meteoroids might be found in asteroids having small semimajor axes and relatively eccentric orbits. (i) The heat sources (such as solar wind–induced currents, ^{26}Al decay, or interasteroid collisions) all increase in effectiveness with decreasing distance to the sun; thus the proportion of differentiated asteroids formed at ≤2 AU should be significantly greater than that formed at greater heliocentric distances (*21*). (ii) The weak gravitational field of Mars is well suited to trap asteroids from elsewhere in the inner solar system into long lifetime ($>10^9$ years) storage orbits, an appreciable number of which will have survived until the present (*10*).

The data of Williams and Hierath [figure 5b in (*20*)] showed that 39 PLS asteroids cross Mars aphelion (~1.7 AU). An additional 35 have perihelia within 0.04 AU of Mars, 47 have perihelia 0.04 to 0.08 AU, and 80 have perihelia 0.08 to 0.12 AU from the orbit of Mars. Impact cratering of these asteroids is most likely near aphelion in the densely populated part of the asteroid belt. To reduce the perihelion by 0.04 AU, the aphelion velocity must be reduced by about 110 m/s. The cumulative number of potential parent asteroids increases rapidly with increasing ejection velocity.

The change in orbital velocity need not occur in a single impact event. After their initial liberation, large (>10 m) meteoroids will collide with comparably sized objects; such events will often involve additional fragmentation. Each of these jostlings will result in changes in the orbital parameters and a random-walk change in these parameters away from those of the parent body. Clearly, the more jostling events a meteoroid has undergone, the greater the mean change in its orbital parameters. On the average, the smaller the meteoroid, the more jostlings it will have experienced.

In summary, both the primary ejection from the parent body and the subsequent collisions with small space debris will cause the orbits of smaller meteoroids to differ more from those of the parent asteroids than do those of larger meteoroids. As a result, the number of parent asteroids providing small debris to the channels that allow escape from the asteroid belt will be greater than the number parental to the large meteoroids reaching these channels. The Antarctic meteorite collection is particularly valuable because it has a much higher efficiency for the collection of these unusual meteoroids having small masses (*22*).

REFERENCES AND NOTES

1. J. T. Wasson, X. Ouyang, J. Wang, E. Jerde, *Geochim. Cosmochim. Acta* **53**, 735 (1989).
2. J. T. Wasson, J. Willis, C. M. Wai, A. Kracher, *Z. Naturforsch. Teil A* **35**, 781 (1980).
3. R. S. Clarke, in *International Workshop on Antarctic Meteorites*, J. O. Annexsted, L. Schultz, H. Wänke, Eds. [Lunar Planet. Inst. Tech. Rep. 86-01 (1986)], pp. 28–29.
4. J. E. Dennison, D. W. Lingner, and M. E. Lipschutz [*Nature* **319**, 390 (1986)] reported a ratio of H to L chondrites in Victoria Land three times that in non-Antarctic falls and finds. A compilation by A. E. Rubin shows a smaller enhancement of 1½ to 2 times compared to finds.
5. M. Prinz, personal communication.
6. I. Halliday and A. A. Griffin, *Meteoritics* **17**, 31 (1982).
7. A. L. Graham *et al.*, *Catalogue of Meteorites* (Univ. of Arizona Press, Tucson, 1985).
8. K. Nishiizumi, D. Elmore, P. W. Kubik, *Earth Planet. Sci. Lett.* **93**, 299 (1989).
9. C. Chang and H. Wänke, in *Meteorite Research*, P. M. Millman, Ed. (Reidel, Dordrecht, Holland, 1969), pp. 397–406.
10. G. W. Wetherill, *Annu. Rev. Earth Planet. Sci.* **2**, 303 (1974).
11. V. F. Buchwald, *Handbook of Iron Meteorites* (Univ. of California Press, Berkeley, 1975).
12. T. Nagata, *Proceedings of the Second Symposium Yamato Meteorites* (National Polar Institute, Tokyo, 1978), p. 70.
13. J. T. Wasson, *Lunar Planet. Sci.* **20**, 1181 (1989).
14. ———, *Meteorites: Their Record of Early Solar-System History* (Freeman, New York, 1985).
15. H. J. Melosh, *Impact Cratering: A Geologic Process* (Oxford Univ. Press, New York, 1989).
16. ———, personal communication.
17. G. W. Wetherill, *Meteoritics* **20**, 1 (1985).
18. D. F. Bender, in *Asteroids*, T. Gehrels, Ed. (Univ. of Arizona, Tucson, 1979), pp. 1014–1063.
19. G. W. Wetherill and J. G. Williams, in *Origin and Distribution of the Elements*, L. H. Ahrens, Ed. (Pergamon, Oxford, 1979), vol. 2, pp. 19–31.
20. J. G. Williams and J. E. Hierath, *Icarus* **72**, 276 (1987).
21. J. T. Wasson and A. E. Rubin, *Nature* **318**, 168 (1985).
22. Without ad hoc augmentations, my model cannot account for the apparent excess of H chondrites in Antarctica; the high abundance of H chondrites in all sets implies that the source body or bodies is near an escape channel, whereas my model accounts for an enhanced flux of meteoroids from bodies distant from the escape channel. My model does predict that the Antarctic set will also prove to have a large fraction of ungrouped stones. Because there is currently no way to correct for pairings resulting from atmospheric breakup, accurate statistics for stones are not yet available.

23. I thank X. Ouyang and L. Zhou for carrying out the neutron activation studies, J. Ma and T. Jen for technical assistance, R. S. Clarke and the U.S. Antarctic Meteorite Committee for samples and documentation, and C. R. Chapman, I. Halliday, A. W. Harris, H. J. Melosh, M. Prinz, A. E. Rubin, G. W. Wetherill, and J. G. Williams for useful discussions. This research was supported by NASA grant NAG 9-40.

17 May 1990; accepted 4 June 1990

Slow Mortality Rate Accelerations During Aging in Some Animals Approximate That of Humans

CALEB E. FINCH, MALCOLM C. PIKE, MATTHEW WITTEN

A general measure of the rate of senescence is the acceleration of mortality rate, represented here by the time required for the mortality rate to double (MRD). Rhesus monkeys have an MRD close to that of humans, about 8 years; their shorter life-span results mainly from higher mortality at all ages. In contrast, some groups with short life-spans (rodents and galliform birds) have shorter MRDs and faster senescence. On the basis of the Gompertz mortality rate model, one may estimate the MRD from the maximum life-span (t_{max}) and the overall population mortality rate. Such calculations show that certain birds have MRDs that are as long as that of humans. These results show that high overall mortality rates or small body sizes do not preclude slow rates of senescence.

ACCELERATIONS OF THE ADULT mortality rate during aging (*1–5*) parallel the increasing incidence of spontaneous degenerative diseases in humans and certain rodents (*6,7*). It is inferred from comparisons of maximum life-spans (t_{max}) that the rate of senescence slowed during evolution in human ancestors, as well as in other mammals (*8–10*). Because t_{max} depends on the acceleration of mortality rate

but also on environmental dangers that may be independent of adult ages, erroneous conclusions about the rate of senescence may be drawn from t_{max} alone.

Many studies indicate that life-span, like other highly plastic life history traits, is subject to selection (*11*); for example, the reversible changes of *Drosophila* life-span during artificial selection for altered reproductive schedules is subject to selection (*12*). Altered life-spans in these lines, however, could result from changes in mortality that were independent of the rate of senescence. One approach to evaluating the relationships between life-span and senescence is to estimate the rate at which mortality accelerates in a population.

Exponential accelerations of mortality rates in humans and certain other animals are shown by graphing the natural logarithm (ln) of mortality rate, $m(t)$, against age. As shown in Figs. 1 and 2, $\ln[m(t)]$ is commonly linear over most of the adult life phase; thus, $m(t)$ is well represented by the Gompertz equation (*1, 2–4, 10*):

$$m(t) = Ae^{\alpha t} \quad (1)$$

where $m(t)$ is the mortality rate at adult age t; α is the rate constant for age-related increases of mortality; and A represents aggregate environmental dangers, for example, from predation, malnutrition, or risky behaviors. With the Gompertz model MRD depends only on α. Solving Eq. 1 for MRD gives

$$\text{MRD} = \ln 2/\alpha \quad (2)$$

Species comparisons in mortality rate accelerations are aided by calculations of the MRD (*2–5*), because MRD changes in the same direction as life-span. Mortality rates may also be described by additional coefficients (Gompertz-Makeham model) (*13*) or by other power functions (Weibull model), in which the MRD changes with age (*14*). Because neonatal mortality rates often vary widely between populations (*1, 3*), we calculate A at puberty, when mortality is least in most feral and domestic populations (*1, 3, 4, 11*), and designate this value as the initial mortality rate (IMR) (*15*).

Despite major differences in overall mortality rates between diverse human populations, MRDs are stable at 7 to 8.5 years, about 30-fold longer than in laboratory rodents (*1–4*). Comparison of different adult human populations show parallel curves of the natural logarithm of mortality [for example, India in 1900 versus Sweden in 1950 (*1, 3*)], which implies that MRD is stable under lifelong adverse or good conditions. Moreover, MRD is also remarkably stable during briefer adversity [for example, concentration camp conditions that caused 30-fold overall increases of mortality rate (*3, 16*) (Fig. 1)]. The provisional assumption that other species also show a resistance of MRD to environmental factors makes it possible for one to compare diverse species without knowing the equivalence of their habitats.

Calculations of MRD and IMR from age-specific mortality data of laboratory populations (Table 1) support previous analyses (*2, 4, 5*). The MRDs of hamsters, mice, and rats are less than 0.5 year and are about 1 year for gerbils and white-footed mice (*Peromyscus*). Values of IMR for inbred mice and rats raised under modern conditions are 10- to 500-fold greater than for larger mammals. Two well-kept colonies of rhesus monkeys (*17, 18*) that had not previously been analyzed for age trends showed MRDS as lengthy as those in humans (Table 1), whereas the IMR for the rhesus monkeys was 100-fold greater than in most human populations. Thus the threefold longer t_{max} of humans compared with rhesus monkeys derives mostly from smaller IMR. This suggests that increases in life expectancy during evolution might result from lowered IMR, as well as from slowed senescence (lengthened MRD), the latter of which was proposed to be the main evolutionary change (*8, 9*). MRDs of certain domestic galliform birds (Fig. 2) lie between values for rodents and dogs but are longer in feral herring gulls (Table 1).

Mortality data for calculating MRDs are often lacking in feral species, and only t_{max} is reported for many birds. Although it is difficult to detect age-related increases in mortality rates in some feral birds with high t_{max} (*19–21*), Botkin and Miller (*22*) showed that the t_{max} is less than that predicted from constant mortality rates. Because short-lived birds clearly show mortality accelerations (Fig. 2), we developed a method

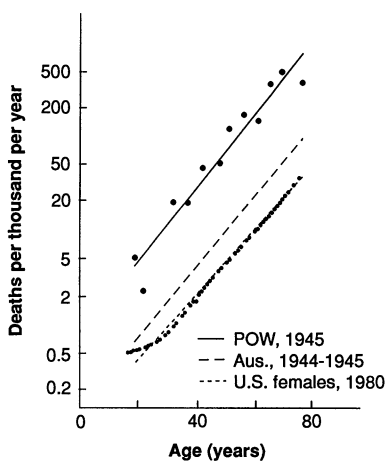

Fig. 1. Mortality rates as a function of age in three human populations (Gompertz mortality rate plots, Eq. 1): POW, Australian prisoners of war in concentration camps of the Japanese Army during World War II (*3, 16*); Aus., civilians in Australia, 1944 to 1945 (*3, 16*); U.S. female, white women in the 1980 U.S. census; the deviations from the line at younger ages could represent effects from cohorts with different values of A or M (*13*). The POW data (*3, 16*) are replotted here for ages up to 75 years. Mortality coefficients for U.S. females are given in Table 1. The slopes (ln α versus age) for the three populations are indistinguishable, whereas IMR ranges tenfold. Similar shifts in IMR with little effect on MRD are shown for Netherlands males during and just after World War II (*3*).

Table 1. Gompertz analysis of mortality rate constants. Calculation from the Gompertz model from mortality rates by age group (Eq. 1, Figs. 1 and 2). IMR was estimated at puberty (Eq. 1); MRD was calculated from the age-related mortality coefficient, α (Eq. 2). Data needed for the analysis of mortality rate changes with age are usually not available in primary form, for example, as mortality schedules by age group or exact life-spans. Most reports present graphs of the fraction surviving as a function of age, from which we extracted average survival by age group. Mortality schedule data were used when available, as indicated. Mortality rates were estimated on the basis of the fraction surviving at each age and were analyzed by linear regression (Figs. 1 and 2). Because these populations were generally small (<100), we did not calculate confidence intervals. These regressions of $\ln[m(t)]$ on t had correlation coefficients that were significant in all cases ($P < 0.05$). In Sacher's (*4*) analysis of dog and horse [data from (*1*)], the values represented only one of several stocks or genotypes; values in Table 1 are averages recalculated for all types of that species in the cited report. Mortality schedules by age group were available for humans, rhesus monkeys, and herring gulls; these data were analyzed according to Eq. 1 on the basis of maximum likelihood estimates, with significance as indicated. The source of data for each species is given in (*33*).

Animal	MRD (years)	IMR/ year	t_{max} (years)
	Mammals		
1. Lab mice	0.27	0.03	4.5
2. Lab rat	0.3	0.002	5.5
3. Lab gerbil	0.9	0.1	3.8
4. Lab hamster	0.5	0.025	3
5. White-footed mouse	1.2	0.06	8
6. Domestic dog	3	0.02	20
7. Horse	4	0.0002	46
8. Rhesus monkey	15	0.02	>35
9. Human	8	0.0002	>110
	Birds		
10. Japanese quail	1.2	0.07	5
11. Reeves pheasant	1.6	0.02	9.2
12. Brush turkey	3.3	0.045	12.5
13. Peafowl	2.2	0.06	9.2
14. Bengal finch	2.5	0.1	9.6
15. Herring gull	5	0.17	49

C. E. Finch, Andrus Gerontology Center and Department of Biological Sciences, University of Southern California, University Park, Los Angeles, CA 90089.
M. C. Pike, Department of Preventive Medicine, University of Southern California Medical School, Los Angeles, CA 90033.
M. Witten, Balcones Research Center, UT System–CHPC, University of Texas, Austin, TX 78758.

to estimate MRD from the average adult mortality rate and t_{max} in the absence of age-specific mortality data.

The proportion of a population surviving from puberty to adult age t, $S(t)$, may be obtained from Eq. 1:

$$S(t) = \exp[(A/\alpha)(1 - e^{\alpha t})] \quad (3)$$

For a population of size N, the age at which the population has diminished to one survivor [$S(t) = 1/N$] approximates t_{max}. Thus,

$$S(t_{max}) \simeq 1/N = \exp\{(A/\alpha)(1 - e^{\alpha t_{max}})\} \quad (4)$$

or

$$t_{max} = \ln[1 + \alpha \ln(N)/A]/\alpha \quad (5)$$

The average mortality rate, A_{av}, of a steady-state population subject to age-specific mortality rates of Eq. 1 is (*23*),

$$A_{av} = 1/\int_0^\infty S(t)dt \quad (6)$$

For a given A_{av}, t_{max}, and N, Eqs. 5 and 6 can be numerically solved for A and α (Table 2). MRDs were calculated for a range of N, because population sizes are unknown. Test populations (Ns) of 10^3 to 10^6 influenced MRD within a two- to three-fold range (Table 2); larger populations, of course, give shorter MRDs. Despite this imprecision, certain conclusions can be drawn. On the basis of mortality data from banding in feral populations, pipestrelle bats show a long MRD (Table 2) that was not expected from the t_{max} and that is as long as in horses (Table 1). The absence of joint degeneration by 19 years in a related bat (*24*) also indicates slow senescence. At least five feral birds also have long MRDs (Table 2). For herring gulls, mortality schedule data also permitted analysis by Eq. 1 (Table 1); thus, the two approaches gave similar MRDs and IMRs. Long MRDs are consistent with slow senecence in marine birds that remain fertile for at least several decades (*21, 25, 26*). Moreover, small size does not preclude a long MRD, as seen in adult pipestrelle bats and certain birds (Table 2). Other analyses (*27*) show that the t_{max} of bats exceeds predictions based on body size from other mammals (*4, 5*) and that body size in general does not rigidly constrain variations in reproductive schedules or lifespans (*28*).

Thus, a short t_{max} from high IMR does not rule out a long MRD. That is, a short t_{max} is still compatible with slow pathophysiological senescence. This result raises concerns about inferences about the rates of senecence from life-span statistics that do not resolve the contributions from mortality accelerations. The long MRDs of many mammals and birds renew questions about rates of senescence in mammalian ancestors (*8, 9*), particularly because Mesozoic placental mammals were rat-sized (*29*). The long MRD of pipestrelle bats weakens predictions from size alone that early mammals necessarily had short t_{max} or rapid senescence. Thus, the fast MRDs of some short-lived rodents and galliform birds could represent independent accelerations of senescence during divergence from more slowly senescing ancestors. Most avian descriptions of fast senescence and short MRD are restricted to galliform birds: chicken (*30*), Japanese quail, Reeves pheasant, brush turkey, and peafowl (Table 1). Domestic chickens show reproductive and other senescent changes by 4 years of age (*30*), which is a decade or more before reproductive declines in many marine birds (*21, 25, 26*). The 50-year lifespan of the Australian echidna (*31*), an egg-laying mammal, implies a long MRD and slow senescence, as does the great t_{max} of some turtles (*1*).

Exponential accelerations of mortality during aging are not usually specified in analyses of life history evolution (*11, 12, 28*) but would require genetic variation to be selectable. Laboratory nematode genotypes that lengthen t_{max} and MRD, but without effect on IMR (*32*), support this possibility. In conclusion, genetic variants influencing IMR and MRD may both be substrates for evolutionary changes in life expectancy.

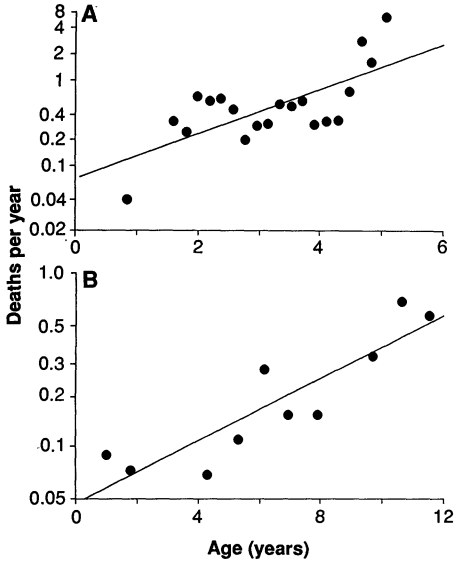

Fig. 2. Mortality rates plotted as a function of age for two short-lived species of birds, (**A**) Japanese quail and (**B**) brush turkey, which show accelerations of mortality that can be fitted by the Gompertz model of mortality (Eq. 1). The age-specific mortality was extracted from survivorship graphs (*1, 38*). Mortality coefficients are in Table 1.

Table 2. Mortality rates estimated in the absence of mortality data by age. Calculation of IMR and α from reported A_{av} and t_{max} (Eqs 5 and 6) (*42*) for populations of different sizes, N. The source of data for each species is given in (*43*).

A_{av}/year	IMR/ year	MRD/ year	t_{max} (years)
1. Pipestrelle bat			
0.36			11
$N = 10^3$	0.25	4.7	
$N = 10^4$	0.22	3.4	
$N = 10^5$	0.20	2.8	
$N = 10^6$	0.19	2.5	
			15
$N = 10^3$	0.32	14.9	
$N = 10^4$	0.28	7.5	
$N = 10^5$	0.26	5.7	
$N = 10^6$	0.25	4.7	
2. European robin			
0.62			12
$N = 10^3$ could not reach t_{max}			
$N = 10^4$	0.58	15.3	
$N = 10^5$	0.54	7.9	
$N = 10^6$	0.52	5.8	
3. Lapwing			
0.34			16
$N = 10^3$	0.30	16.4	
$N = 10^4$	0.27	8.2	
$N = 10^5$	0.25	6.0	
$N = 10^6$	0.24	5.1	
4. Starling			
0.52			20
$N = 10^{3-4}$ could not reach t_{max}			
$N = 10^5$	0.51	56.6	
$N = 10^6$	0.49	21.2	
5. Common swift			
0.18			21
$N = 10^3$	0.12	8.2	
$N = 10^4$	0.10	6.0	
$N = 10^5$	0.094	5.1	
$N = 10^6$	0.088	4.5	
6. Herring gull			
0.04			49
$N = 10^3$	0.0060	7.2	
$N = 10^4$	0.0046	6.3	
$N = 10^5$	0.0037	5.7	
$N = 10^6$	0.0032	5.4	

REFERENCES AND NOTES

1. A. Comfort, *The Biology of Senescence* (Elsevier, New York, ed. 3, 1979).
2. T. B. L. Kirkwood, in *Handbook of the Biology of Aging*, C. E. Finch and E. L. Schneider, Eds. (Van Nostrand, New York, ed. 2, 1985), pp. 27–44.
3. H. B. Jones, *Adv. Biol. Med. Phys.* **4**, 281 (1956); in *Handbook of Aging and the Individual*, J. E. Birren, Ed. (Univ. of Chicago Press, Chicago, 1959), pp. 336–363.
4. G. S. Sacher, in *Handbook of the Biology of Aging*, C. E. Finch and L. Hayflick, Eds. (Van Nostrand, New York, ed. 1, 1977), pp. 582–638.
5. W. A. Calder III, *Size, Function, and Life History* (Harvard Univ. Press, Cambridge, MA, 1984).
6. H. S. Simms and B. N. Berg, *J. Gerontol.* **12**, 244 (1957).
7. P. J. Cook *et al.*, *Int. J. Cancer* **4**, 93 (1969).
8. R. G. Cutler, *J. Hum. Evol.* **5**, 169 (1976); *Gerontology* **25**, 69 (1980).
9. M. A. Hofman, *Q. Rev. Biol.* **58**, 495 (1983).
10. B. L. Strehler, *Time, Cells, and Aging* (Academic Press, New York, ed. 2, 1977).
11. G. C. Williams, *Evolution* **11**, 398 (1957); W. D. Hamilton, *J. Theor. Biol.* 7, 1 (1964); B. Charlesworth, *Evolution in Age-Structured Populations* (Cambridge Univ. Press, Cambridge, 1980); M. R. Rose and J. L. Graves, Jr., *J. Gerontol.* **44**, B27 (1989).
12. L. S. Luckinbill *et al.*, *Evolution* **38**, 996 (1984); L. D. Mueller, *Proc. Natl. Acad. Sci. U.S.A.* **84**, 1974 (1987); P. M. Service *et al.*, *Evolution* **42**, 708 (1988).
13. In addition to the coefficient A in Eq. 1, which represents a constant proportion of the exponential

increase of mortality with age, the Gompertz-Makeham model adds the age-independent Makeham constant (M): $m(t) = Ae^{\alpha t} + M$ (*1, 4, 10*). The constant M has diminishing effect on $m(t)$ as age advances, so that the slope of $\ln[m(t)]$ becomes progressively steeper (*4*). Because A is in fixed proportion to the exponential increase of mortality, variations in A between populations yield parallel lines of $\ln[m(t)]$ on age (*3*). Analyses that discriminate contributions from A and M in real populations are lacking. The simpler model (Eq. 1) fits the data analyzed here over most adult ages (Figs. 1 and 2). Because the primary mortality schedule data across the life-span are rarely reported, age group average mortality rates must be extracted from survivorship graphs. Consequently, analyses of mortality rate changes with age are first approximations that are best addressed by the simplest model.

14. As alternatives to the Gompertz model (Eq. 1), power functions such as the Weibull model are used to describe population senescence: $m(t) = At^{c-1}$ [M. Witten, in *Evolution of Longevity in Animals: A Comparative Approach*, A. D. Woodhead and K. H. Thompson, Eds. (Plenum, New York, 1987), pp. 295–318]. As shown for several invertebrates [H. R. Hirsch and B. Peretz, *Mech. Ageing Dev.* **27**, 43 (1984); W. Slob and C. Janse, *ibid.* **42**, 275 (1988)], the fit of the Gompertz and Wiebull formulas varies between populations. Graphs of $\ln[m(t)]$ against age give a straight line with the Gompertz but a concave curve with the Weibull. The MRD does not depend on age with the Gompertz but declines slightly at later ages with the Weibull because of its concave form on semilogarithmic plots. This outcome makes species comparisons of mortality acceleration less awkward with the Gompertz than with the Weibull. Because we have equated aging with MRD, use of the Weibull would necessitate comparing "average" MRDs; these averages would be close to the MRDs calculated from the Gompertz, because a fitted Gompertz straight line approximates a fitted Weibull curve.
15. Because A and α may not be independent (*10*), we emphasize the empirical value of an initial mortality rate (IMR) for A. Calculation of A at puberty seems a more meaningful basis for comparing species than that extrapolated to birth ($t = 0$) when mortality is often high and more variable between populations. Moreover, calculations of A (*2, 4*) extrapolated to $t = 0$ at birth underestimate A during the adult phase when mortality rate begins to increase exponentially in populations. Except for a few domestic and laboratory animals, mortality data are not available by age across the adult life-span for calculating MRDs. Further analysis of relationships between α and A are given by Johnson (*32*).
16. R. A. M. Bergman, *J. Gerontol.* **3**, 14 (1948).
17. B. Dyke *et al.*, *Am. J. Primatol.* **10**, 257 (1984).
18. J. Tigges *et al.*, *ibid.* **15**, 263 (1988).
19. S. T. Buckland, *J. Anim. Ecol.* **51**, 833 (1982).
20. D. Lack, *The Natural Regulation of Animal Numbers* (Oxford Univ. Press, New York, 1954).
21. J. C. Ollason and G. M. Dunnet, in *Reproductive Success: Studies of Individual Variation in Courtship Breeding Systems*, T. H. Clutton-Brock, Ed. (Univ. of Chicago Press, Chicago, 1988), pp. 263–278.
22. D. B. Botkin and R. S. Miller, *Am. Nat.* **108**, 181 (1974). This approach also included an examination of a model wherein mortality rates increased as a linear function of age, a mortality function that has not been documented from detailed mortality schedules.
23. E. J. Gumbel, *Statistics of Extremes* (Columbia Univ. Press, New York, 1958).
24. L. Sokoloff, *The Biology of Degenerative Joint Disease* (Univ. of Chicago Press, Chicago, 1969).
25. J. C. Coulson and J. Horobin, *J. Anim. Ecol.* **35**, 269 (1976).
26. B. H. Pugasek, *Behav. Ecol. Sociobiol.* **13**, 161 (1983).
27. K. D. Jürgens and J. Prothero, *Comp. Biochem. Physiol. A* **88**, 361 (1987).
28. J. S. Millar and R. M. Zammuto, *Ecology* **64**, 631 (1983); B. E. Saether, *Nature* **331**, 616 (1988); A. F. Read and P. D. Harvey, *J. Zool. London* **219**, 329 (1989); D. E. L. Promislow and P. H. Harvey, *ibid.* **220**, 417 (1990).
29. R. L. Carroll, *Vertebrate Paleontology and Evolution* (Freeman, New York, 1988).
30. J. A. Barr and S. S. Palmer, *Poultry Biol.* **2**, 103 (1989); M. A. Ottinger *et al.*, *Hormones Behav.* **17**, 197 (1983); J. B. Williams and P. J. Sharp, *J. Reprod. Fertil.* **53**, 141 (1978). No mortality schedule data are reported for domestic chickens.
31. R. M. Nowak and J. L. Paradiso, *Walker's Mammals of the World* (Johns Hopkins Univ. Press, Baltimore, ed. 4, 1983).
32. T. E. Johnson, *Proc. Natl. Acad. Sci. U.S.A.* **84**, 3777 (1987); *Science* **249**, 908 (1990).
33. The data presented in Table 1 are from the following sources. Mammals. 1. Mouse (*Mus musculus*): Average of values calculated for females of six long-lived inbred mouse strains at the Jackson Laboratory. Age-group data were taken from graphs of mortality rate on age (*34*) and represent seven to nine adult age groups and >600 mice per strain: A/J (IMR, 0.024/year; MRD, 0.26 year); CBA/J (0.027/year; 0.26 year); C57BL/6J (0.025/year; 0.30 year); DBA/2J (0.008/year; 0.26 year); SJL/J (0.073/year; 0.26 year); 129/J (0.02/year; 0.28 year). Regressions were significant at $P < 0.01$–0.001. Values for MRD were statistically indistinguishable. Overall mean ± SEM (n = 6 strains): IMR, 0.03 ± 0.01/year; MRD, 0.27 ± 0.008 year. 2. Rat (*Rattus norvegicus*): Data calculated from mortality schedules of Fischer 344 male rats, fed ad libitum (*35*). 3. Gerbil (*Meriones unguiculatus*): Data from (*36*). 4. Hamster (*Mesocricetus aureus*): Data from (*37*). 5. White-footed mouse (*Peromyscus leucopus*): IMR was recalculated at puberty from (*4*). 6. Domestic dog (*Canis familiaris*): Average of four breeds: cocker spaniel (IMR, 0.004/year; MRD, 2.4 years); pekinese (0.012/year; 3.1 years); mastiff (0.012/year; 2 years); wolfhound (0.044/year; 4 years). Data from (*1*). 7. Horse (*Equus caballus*): Average of thoroughbred mare (IMR, 0.0002/year; MRD, 4.5 years) and Arabian mare (0.0002/year; 3.8 years). Data from (*1*). 8. Rhesus monkey (*Macaca mulatta*): Calculated from mortality schedule data by Eq. 1 as maximum likelihood estimates. Average of values for two populations aged 4.5 to 24.5 years. Monkeys born at the Wisconsin Regional Primate Center; data from (*17*), table II, column q(x), that represent spontaneous deaths and excludes monkeys removed for experimentation (B. Dyke, personal communication); data were combined for males and females: IMR, 0.02/year; MRD, 18 years ($P < 0.01$). Feral-born monkeys brought at about 2 years of age to the Yerkes Regional Primate Center; data from (*18*), table I, that present the combined genders: IMR, 0.02/year; MRD, 12 years ($P < 0.01$); t_{max} from (*18*) may be expected to increase further. 9. Human, U.S. white females in 1980. Data from U.S. Department of Health and Human Services Life Tables calculated by Eq. 1 as maximum likelihood estimates ($P < 0.001$). Jones's (*3*) analysis of populations throughout the world during the 19th to mid-20th centuries indicates a remarkable consistency of MRD, 7 to 8.5 years, despite severalfold differences in life expectancy that reflect varying impacts of infectious diseases and malnutrition. The human t_{max} is uncertain, because indisputable birth records and lifelong identification are not available before about 1880.

    Birds (mortality data by age group are not available for domestic chickens). 11. Japanese quail, male (*Coturnix coturnix japonica*): Data from laboratory populations (*38*). Feral quail have similarly short t_{max} (*39*); California quail (*Lophortyx californica*), 6.8 years; Gambel's quail (*L. gambeli*), 7.4 years. 12. Reeves pheasant (*Syrmaticus reevesi*): London Zoo, data from (*1*). 13. Brush turkey (*Alectura lathami*): London Zoo, data from (*1*). 14. Peafowl (*Pavo cristatus*): London Zoo, data from (*1*). 15. Bengal finch, female (*Lonchura striata*): London Zoo, data from (*1*). 16. Herring gull (*Larus argentatus*): Age group mortality data from banding studies of feral populations (*40*) analyzed according to Eq. 1 by the method of maximum likelihood ($P < 0.01$) gave mortality rate coefficients in good agreement with the analysis by Eqs. 5 and 6 (Table 2); t_{max} from (*41*).
34. J. B. Storer, in *Genetic Effects on Aging*, D. Bergsma and D. E. Harrison, Eds. (Liss, New York, 1978), pp. 55–70.
35. B. Y. Yu *et al.*, *J. Gerontol.* **37**, 130 (1982).
36. G. M. Troup *et al.*, *Exp. Gerontol.* **4**, 139 (1969).
37. E. Stuchlíková *et al.*, *ibid.* **10**, 141 (1975).
38. A. Cherkin and M. J. Eckhardt, *J. Gerontol.* **32**, 38 (1977); A. E. Woodard and H. Abplanalp, *Poultry Sci.* **50**, 688 (1971).
39. R. B. Clapp *et al.*, *J. Field Ornithol.* **53**, 81 (1982).
40. E. S. Deevey, Jr., *Q. Rev. Biol.* **22**, 283 (1947).
41. T. G. Pearson, *Bird Lore* **37**, 412 (1935).
42. When mortality rate data by age group were unavailable, calculations were based on Eq. 2 according to the following procedure in which we used A_{av}, the reported (average) population mortality rate from banding and recapture studies, and t_{max}, either from banding and recapture or from captive specimens [see notes for individual species in (*43*)]. A computer program fitted values of A and α for Eq. 2 so as to be consistent with reported A_{av} and t_{max} for populations of different sizes. In Eqs. 1 and 6, A must always be less than A_{av}, because the latter represents contributions from both A and α. The program integrated $S(t)$ from 0 to twice t_{max}. The algorithm used a series of values for A (20 steps from 0.001 to 0.999 of the value of A_{av}) to estimate α for each trial A_0, so as to minimize the difference between the entered A versus the A calculated for each trial A_0 and the estimated α. Before proceeding from one trial A to the next, the program calculated t_{max} using the current trial A_0 and α, and compared its value to the entered t_{max}. If the difference did not exceed a specified tolerance percentage, the current trial A and α were accepted. However, if the best trial did not reach the accepted tolerance for t_{max} at that population size, then a new series of trial A values was defined to fall between the best two values for the current trial A. Trial A and α values were iteratively fitted in this manner for successively larger populations, $10^{N = 3, 4, 5, 6}$. These calculations require no assumptions about the relation of body size to the mortality coefficients. Calder (*5*) derived Eq. 5 for calculations of life expectancy as a function of body size.

    These calculations also show that some of values of A_{av} assumed by Botkin and Miller (*22*) did not permit the reported t_{max}. For example, A_{av} = 0.2/year for the arctic tern is incompatible with survival to the observed t_{max} of 31.2 years with population sizes up to 10^6; a lower estimate of A_{av} = 0.1/year permits this t_{max} and may be more realistic. This analysis thus gives a validation of A_{av} and t_{max} from banding-recapture studies.
43. The source of data for each species in Table 2 is given by species as numbered. In all cases A_{av} and t_{max} were obtained from banding studies of feral populations. 1. Pipestrelle bat (*Pipestrellus pipestrellus*) (sp): A_{av} (*44*); body adult weight, ≤20 g (*31*). Two calculations were made on the basis of different t_{max}: the t_{max} of 11 years (*44*) may be a considerable understimate, in view of the longer life-spans of other small vespertilionids, for example, *P. subflavus* (20 g, 14.8 years) (*31*) and *Myotis lucifugis* (8 g, >30 years) (*27, 31, 44*). We therefore also made calculations assuming a more likely t_{max} of 15 years. The data for mortality by age group (*44*) were also analyzed by Eq. 1; although the regression analysis did not achieve significance, the estimated mortality coefficients were close to those from Eqs. 5 and 6: IMR, 0.25/year; MRD, 8 years. 2. European robin (*Erithacus rubecula*): A_{av} and t_{max} (*22*); body weight, 16 g (*5*). 3. Lapwing (*Vanellus*): A_{av} and t_{max} (*22*); body weight, 220 g (*5*). 4. Starling (*Sternus vulgaris*): A_{av} and t_{max} (*22*); body weight, 75 g (*5*). 5. Common swift (*Apus apus*): A_{av} and t_{max} (*21*); body weight, 40 g (*5*). 6. Herring gull (*Larus argentatus*): A_{av} (*21*); t_{max} (*41*); body weight, 950 g (*5*). Data on mortality rates by age group were analyzed by Eq. 1 (see Table 1) and agree with these results. Numerous other bird species survive at least 20 to 30 years (*1, 21, 22, 39*).
44. M. J. A. Thompson, *J. Zool. London* **211**, 209 (1987).
45. This research was supported by the John D. and Catherine T. MacArthur Foundation Network in Successful Aging. We are grateful for comments given during preparation of the manuscript by S. Austad, W. Fitch, T. Johnson, J. Phelan, J. Prothero, J. Nesselroade, R. Rickleffs, M. Rose, B. Strehler, and M. Waterman.

2 October 1989; accepted 23 May 1990